

LETTERS

Narrow Mie Optical Cavity Resonances from Individual 100 nm Hematite Crystallites

Stanislaus S. Wong and Louis E. Brus*

Columbia University, Department of Chemistry, Havemeyer Hall, 3000 Broadway, New York, New York 10027

Received: July 19, 2000; In Final Form: November 8, 2000

Rhombohedral single crystallites of hematite (iron oxide, $\alpha\text{-Fe}_2\text{O}_3$) in the size range of 20–200 nm have been synthesized by forced hydrolysis in water. The optical Rayleigh scattering and AFM topography of individual crystallites have been recorded on an inverted microscope based apparatus. Individual crystallites show narrow Mie “optical cavity” resonances across the visible spectrum as the particle size increases. These spectra are far sharper than the size broadened extinction spectra of the parent colloid. In the blue region near the intense band gap optical absorption, the resonances are also significantly sharper than calculated from simple scattering theory. This unexpected structure is discussed in terms of single crystallite birefringence, and uncertainties in hematite bulk optical properties.

Introduction

The study of the synthesis of colloidal dispersions composed of particles of uniform size and shape has been of great and enduring interest.^{1,2} Not only are these systems³ aesthetically appealing but also they serve as model systems for understanding optical, magnetic, electrokinetic, and adsorptive properties of bulk matter because of their narrow size distribution and well-defined geometry and structure. The applications of this research can be found in the design of electromagnetic devices, catalysts, photosensitive materials, medicines, pigments, and ceramics.

In this study, we synthesize and characterize single hematite (iron oxide, $\alpha\text{-Fe}_2\text{O}_3$) crystallites. Hematite is present in highly weathered soils and is found in the clay fraction of tropical and subtropical soils, giving them their pink bright red hue. Bacteria in surface waters are known to catalyze the oxidation of magnetite to hematite.⁴ Hematite present in soil is thought to be catalytic in the oxidation of chlorinated pollutants in groundwater. Furthermore, hematite is also found in cosmic dust

as well as in natural atmospheric and polluted aerosols. Hence, understanding the optical and scattering properties⁵ of hematite leads to insight into the radiative effects of atmospheric aerosols on the radiative energy balance of the earth-atmosphere system. Rapid and accurate determination of particle size and shape is also critical in understanding processes responsible for phenomena involving the formation of metal oxides such as metal corrosion.⁶

¹Dielectric particles show a Mie scattering resonance when the diameter d is on the order of one-half an internal optical wavelength. In hematite, this occurs at about $d = 80$ nm for 5000 Å blue-green light, because the index of refraction is very high, i.e., 2.9. This purely electromagnetic effect occurs at sizes about an order of magnitude larger than the quantum mechanical size effect extensively studied in semiconductors such as CdSe. Hematite is actually best described as a narrow band Mott charge-transfer insulator; it can be doped, but electrons and holes are self-trapped with very low reported mobilities.⁷ A particle showing a Mie resonance heuristically is a micro-optical cavity with an intensified optical field both inside and near the particle surface. This intensification can lead to enhanced Raman

* To whom correspondence should be addressed. Tel: 1-212-854-4041. Fax: 1-212-932-1289. E-mail: brus@chem.columbia.edu.

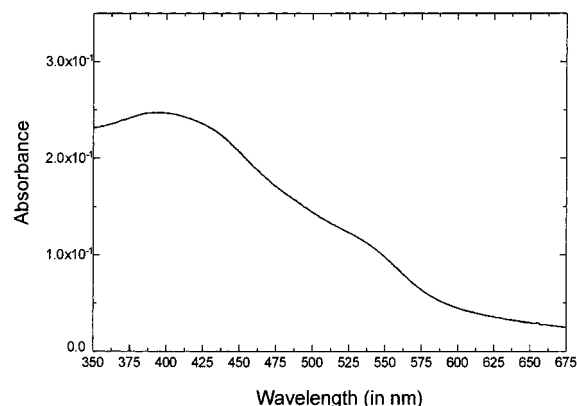


Figure 1. Extinction spectrum of hematite nanocrystals, prepared after 7 days of incubation at 100 °C.

scattering, as shown by organic molecules adsorbed on noble metals. Hematite Mie resonances have been previously reported⁶ in colloidal extinction spectra that were inhomogeneously broadened by the sample size and shape distribution. In this paper, we study Mie resonances in single crystalline hematite particles, as a first step toward developing sensitive optical methods for monitoring aqueous surface reactions.

Experimental Methods and Synthesis

Preparations of monodisperse hematite particles of different sizes and morphologies are known. The mechanism⁸ is forced hydrolysis; a burst of nuclei is produced and allowed to grow uniformly, resulting in particles with narrow size distribution.⁹ At 100 °C, many polyvalent metal ions readily hydrolyze¹⁰ and deprotonation of coordinated water molecules is accelerated. Amorphous iron hydroxides quickly form, and slowly convert to hematite single crystallites over a period of days. Anions, such as phosphate ions that strongly coordinate to dissolved metal ions, have been used to control shape in the formation of ellipsoidal particles of varying axial ratio.^{11,12}

Following the earlier work of Matijevic¹ and Serna,¹³ 100 cm³ of 0.02 M FeCl₃ aqueous solutions under air in closed containers were aged at 100 °C for periods of 1 day, 2 days, and 7 days, respectively. Over this time, the color of the suspension evolves from light orange to dark red. The color of the suspension depends on the particle size and shifts to darker hues with increasing diameter, due to greater absorption of light in the blue-green range of the spectrum.¹⁴ At 7 days, the extinction spectrum in Figure 1 shows a broad peak near 400 nm, with a shoulder near 550 nm.

In addition, to generate rodlike, elliptically shaped particles,^{10,15} 0.02 M FeCl₃ aqueous solutions were incubated in the presence of 0.0005 M KH₂PO₄ for a period of a week; particles produced had aspect ratios of up to 7:1.

Our inverted microscope based, optical scattering CCD apparatus has been described.¹⁶ We previously used this apparatus to obtain the dark field Rayleigh scattering (Mie) spectra of individual Ag nanocrystals. The incident white light is unpolarized; scattering is observed with a NA 0.55 objective at an angle of approximately 60° with respect to the forward scattering direction. To directly measure the morphology of the same crystallite observed in the dark field Mie scattering, we have incorporated a Digital Instruments (Santa Barbara, CA) Bioscope AFM, equipped with a Nanoscope IIIa controller. The scanning head of the AFM can be mounted over the fixed quartz coverslip on the microscope, after the dark field condenser and

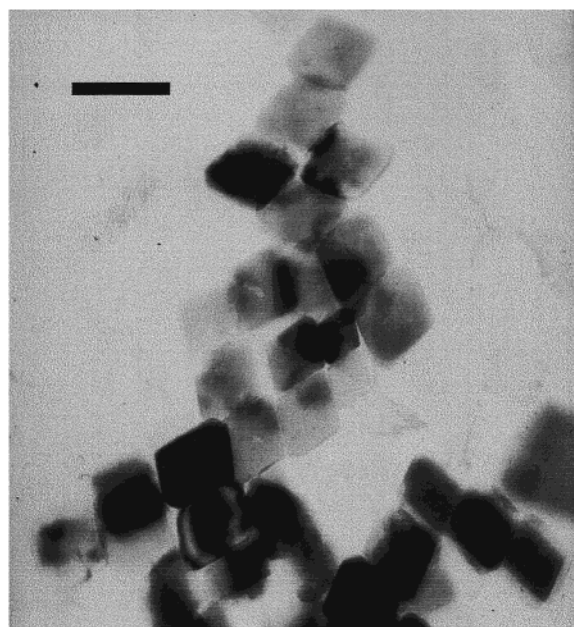


Figure 2. TEM micrograph of hematite nanocrystals, prepared after 7 days of incubation at 100 °C. Scale bar represents 125 nm.

lamp have been removed from the microscope stage. Tapping mode AFM images are obtained in air with FESP (force modulation etched silicon probes) and TESP (tapping mode etched silicon probes) with force constants of 0.1–10 N/m. Nanocrystal samples were prepared by spin coating onto a quartz microscope coverslip.

Results and Discussion

Hematite is a rhombohedral crystal of the corundum structure, similar to sapphire.^{17,18} TEM examination, in Figure 2, shows rhombohedrally shaped, crystalline faceted large single nanocrystals. A typical size is 80 nm after 2 days and 120 nm after 7 days. Nanocrystals tend to self-organize as the solution dries on the TEM grid. A few crystallites are aligned to strongly diffract the electron beam and appear black in this Figure. Strain fields are apparent for several touching particles. X-ray powder patterns of precipitated crystallites show only the expected strong lines of hematite.¹⁹

The particles probably have adsorbed surface chloride. However, on the basis of the data and characterization evidence collected, it is certain that the hematite prepared is stoichiometrically pure in bulk. As samples were prepared in an oxidizing environment and analyzed in equilibrium with moist air, the surface hematite stoichiometry should remain unchanged. That is, the surface should be completely oxidized.

Most of the particles examined by AFM on the quartz coverslip are aggregated. The individual rhombohedral particles typically have a height that is one-half or one-third of the in-plane length and width dimension. This synthesis makes slightly oblate crystallites that lie flat on surfaces. We presume that the crystallites have a short hexagonal *c*-axis, perpendicular to the plane in the TEM and optical images. The in-plane length/width ratio of the particles observed in AFM is 1.15 on average, in agreement with the value derived from the TEM results.

If the hematite nanocrystals are separated by 1 μm or more on the quartz coverslip, then the tungsten lamp dark field scattering by individual particles can be seen through the eyepiece, and also recorded on the CCD camera in imaging and/or spectroscopic modes. While most scattering points appear

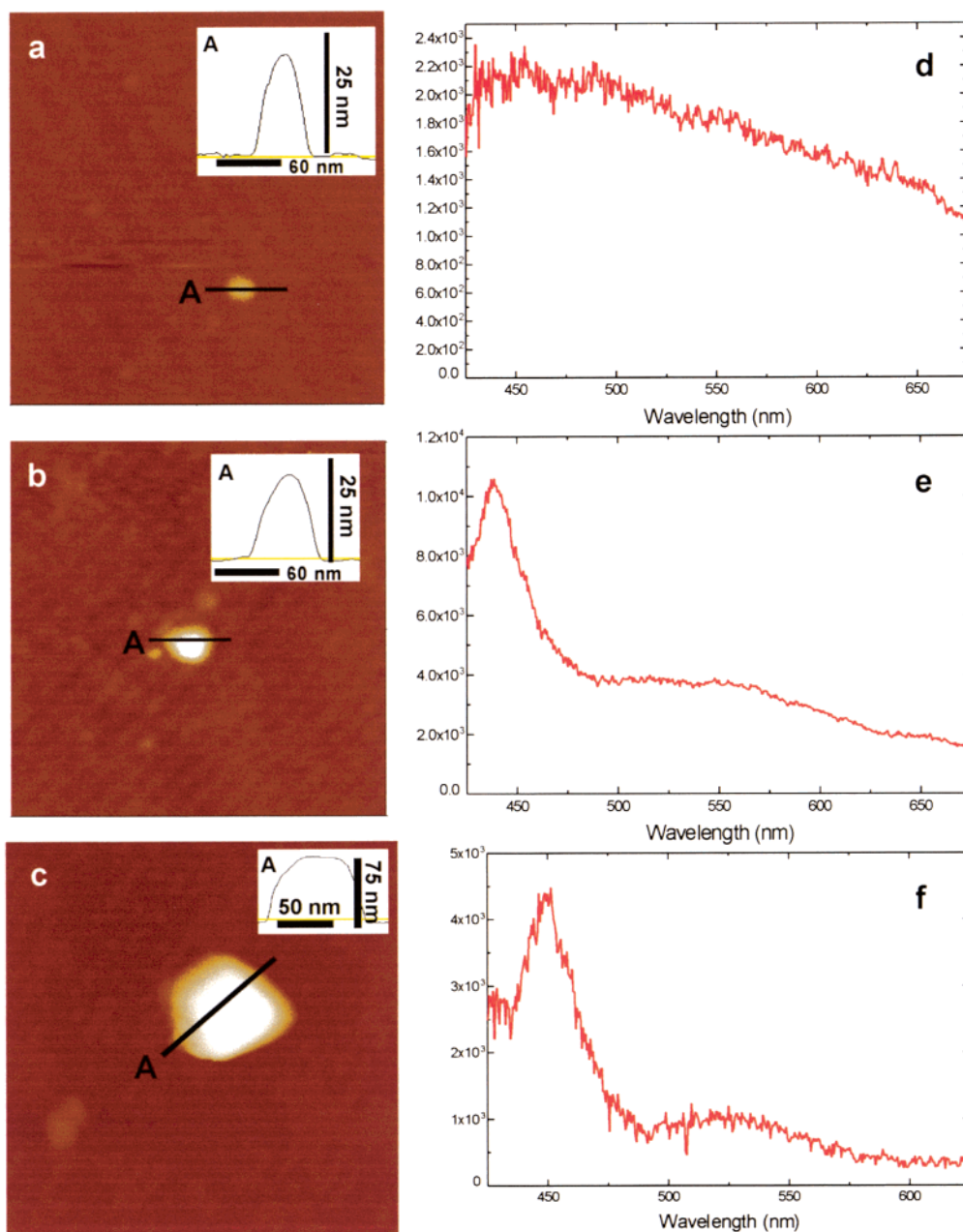


Figure 3. Parts a through c are AFM height images, measuring 500 nm by 500 nm, of increasingly larger hematite nanocrystals. (Inset) Cross-section drawn across each particle, representing a line cutting through the nanocrystal at point A. Heights at half-maximum for the particles are for parts a–c: 8.9, 9.7, and 37.6 nm, respectively. Parts d–f represent Mie scattering images of the corresponding hematite nanocrystals.

white and thus have broad Rayleigh scattering, about 10% show a distinct color to the eye, with a structured Mie scattering spectrum, as shown in Figures 3 and 4. AFM examination shows that these are single, nonaggregated nanocrystals.

The larger individual particles often show rather sharp scattering resonances, that tend to shift from blue to red as size increases. Figure 3a shows a small particle without a resonance. Figures 3b,c and 4a show somewhat larger particles with sharp resonances in the blue. Figure 4b shows the red resonance of a rather large particle. Figure 4c presents a broadened resonance of a dimer particle, composed of two smaller particles with individual resonances in the blue. As expected, the single nanocrystal scattering spectra are sharper than the Figure 1 extinction spectra of the size-broadened parent colloid but can be visualized as essentially discrete, constituent components of that Figure.

We have attempted to fit these spectra using the same wavelength-dependent index of refraction data derived by Kerker et al., and used by Hsu and Matijevic,⁶ in fitting their size broadened colloidal extinction spectra. We have used the analytical Mie theory²⁰ for spheres, as well as the numerical T-matrix programs developed by Barber and co-workers^{21,22} for oblate ellipsoids of revolution. As shown in Figure 5 for spherical particles, these calculations reproduce the shift from blue to red with increasing size though they do not express the sharp blue resonances we observe. As well, the calculations do produce red Mie resonances in rough agreement with our observations. Similar trends are observed with oblate-shaped particles as has been observed previously in thin film studies.²³ Agreement with experiment is not improved if we use the dielectric data of Chen and Cahan²⁴ instead of the Kerker et al.²⁵ index data.

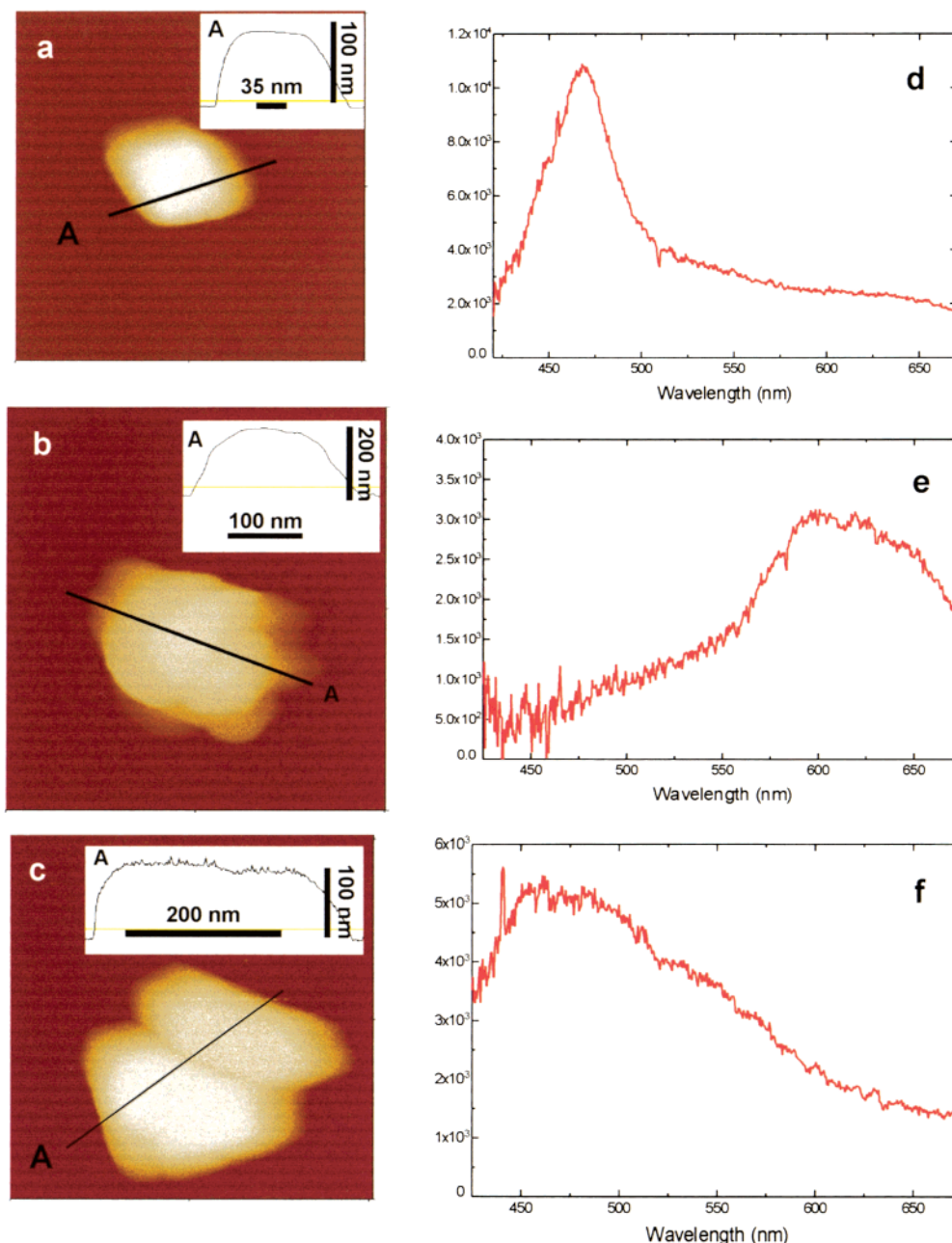


Figure 4. Parts a and b are AFM height images, measuring 500 nm by 500 nm, of increasingly larger hematite nanocrystals. Part c is the corresponding AFM height image (500 nm by 500 nm) of a dimer hematite particle. (Inset) Cross-section drawn across each particle, representing a line cutting through the nanocrystal at point A. Heights at half-maximum for the particles are for parts a–c: 61.8, 116, and 62.9 nm, respectively. Parts d–f represent Mie scattering images of the corresponding hematite nanocrystals.

Hematite is birefringent with a unique *c*-axis. This birefringence is neglected in the Mie calculations, which use an average isotropic index of refraction. The oblate rhombohedral nanocrystals appear to have their *c*-axis perpendicular to the substrate, and are aligned with respect to the incoming white light. Perhaps, an interference effect involving birefringence is involved in this discrepancy.

A more likely possibility, though, is that both sets of complex, wavelength-dependent hematite dielectric data^{24,25} are inaccurate in the blue region of strong absorption. Hematite has a strong charge-transfer optical absorption ('band gap') in the blue where we see an unexpected resonance. At longer wavelengths, hematite is essentially transparent with a real optical index of about 3.0—in this region, the optical properties are not in question. As the charge-transfer absorption is approached from

lower energy, the optical dielectric constant shows resonance,²⁶ presumably corresponding to a maximum in the energy density within the dielectric hematite particle. The imaginary part increases and the real part decreases after reaching a peak of 11 at 577 nm. It may be that the real part becomes very small or even negative. The type of pronounced blue resonance we see is reminiscent of the resonance observed in small Ag particles, associated with the excitation of surface resonance plasmons,²⁷ where a negative real part of the complex refractive index does indeed exist.

Acknowledgment. We thank Stephen P. O'Brien for TEM studies and help with X-ray diffraction work, Amy M. Michaels for Mie scattering computing algorithms, and Enrique R. Batista for help with using T-matrix methods. The financial support of

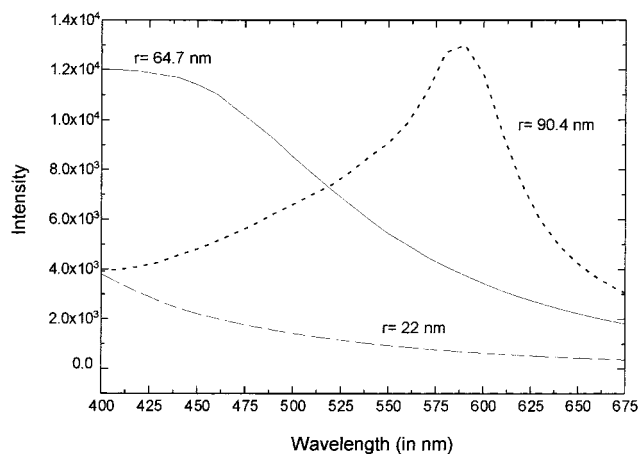


Figure 5. Simulated extinction spectra of spherically shaped hematite nanocrystals with radii of 22 (dotted line composed of short segments), 64.7 (solid line), and 90.4 (dotted line composed of long segments) nm, respectively.

the Environmental Molecular Sciences Institute (EMSI) at Columbia University is gratefully acknowledged. We have also used facilities supported by the Columbia MRSEC under NSF MRSEC Grant #DMR-98-09687.

References and Notes

- (1) Matijevic, E. *Chem. Mater.* **1993**, *5*, 412.
- (2) Matijevic, E. *Langmuir* **1986**, *2*, 12.
- (3) Matijevic, E. *Acc. Chem. Res.* **1981**, *14*, 22.

- (4) Brown, D. A.; Sherriff, B. L.; Sawicki, J. A. *Geochim. Cosmochim. Acta* **1997**, *61*, 3341.
- (5) Mita, A.; Isono, K. *J. Meteorol. Soc. Jpn.* **1980**, *58*, 69.
- (6) Hsu, W. P.; Matijevic, E. *Appl. Opt.* **1985**, *24*, 1623.
- (7) Brown, G. E.; Henrich, V. E.; Casey, W. H.; Clark, D. L.; Eggleston, C.; Felmy, A.; Goodman, D. W.; Gratzel, M.; Maciel, G.; McCarthy, M. I.; Nealon, K. H.; Sverjensky, D. A.; Toney, M. F.; Zachara, J. M. *Chem. Rev.* **1999**, *99*, 77.
- (8) Privman, V.; Goia, D. V.; Park, J.; Matijevic, E. *J. Colloid Interface Sci.* **1999**, *213*, 36.
- (9) Lamer, V. K.; Dinegar, R. H. *J. Am. Chem. Soc.* **1950**, *72*, 4847.
- (10) Ocana, M.; Morales, M. P.; Serna, C. J. *J. Colloid Interface Sci.* **1995**, *171*, 85.
- (11) Ishikawa, T.; Matijevic, E. *Langmuir* **1988**, *4*, 26.
- (12) Ozaki, M.; Kratochvil, S.; Matijevic, E. *J. Colloid Interface Sci.* **1984**, *102*, 146.
- (13) Ocana, M. J.; Rodriguez-Clemente, R.; Serna, C. J. *Adv. Mater.* **1995**, *7*, 212.
- (14) Penners, N. H. G.; Koopal, L. K. *Colloids Surf.* **1986**, *19*, 337.
- (15) Morales, M. P.; Gonzalez-Carreño, T.; Serna, C. J. *J. Mater. Res.* **1992**, *7*, 2538.
- (16) Michaels, A. M.; Nirmal, M.; Brus, L. E. *J. Am. Chem. Soc.* **1999**, *121*, 9932.
- (17) Pauling, L.; Hendricks, S. B. *J. Am. Chem. Soc.* **1925**, *47*, 781.
- (18) Blake, R. L.; Hessevick, R. E. *Am. Mineral.* **1966**, *51*, 123.
- (19) Clarke, N. S.; Hall, P. G. *Langmuir* **1991**, *7*, 672.
- (20) Mie, G. *Ann. Phys.* **1908**, *25*, 377.
- (21) Hill, S. C.; Hill, A. C.; Barber, P. W. *Appl. Opt.* **1984**, *23*, 1025.
- (22) Barber, P. W.; Hill, S. C. *Light Scattering by Particles: Computational Methods*; World Scientific: NJ, 1990.
- (23) Ryde, N. P.; Matijevic, E. *Appl. Opt.* **1994**, *33*, 7275.
- (24) Chen, C. T.; Cahan, B. D. *J. Opt. Soc. Am.* **1981**, *71*, 932.
- (25) Kerker, M.; Scheiner, P.; Cooke, D. D.; Kratochvil, J. P. *J. Colloid Interface Sci.* **1979**, *71*, 176.
- (26) Bennett, H. S.; Rosasco, G. J. *Appl. Opt.* **1978**, *17*, 491.
- (27) Bohren, C.; Huffman, D. *Absorption and Scattering of Light by Small Particles*; Wiley: New York, 1983.